

Supporting Information for:

**Coordination-driven Self-assembled Mn(II)-Metallostar
Endowed with High Relaxivity and Synergistic Photothermal
and Photodynamic Effects**

Huiyu Wu,^{1,2,§} Zhenghui Li,^{1,4,§} Yao, Liu,^{1,3} Xingchi Shi,⁵ Yuan Xue,^{1,3} Zuhua Zeng,^{1,2} Fanglin, Mi,⁴ Haiying Wang^{1,*}
and Jiang Zhu^{1,*}

¹ Medical Imaging Key Laboratory of Sichuan province, Department of Oncology, Affiliated Hospital of North Sichuan Medical College, Maoyuan Road 1, Nanchong City, Sichuan, 637000, China.

² School of Pharmacy, North Sichuan Medical College, Fujiang Road 234, Nanchong City, Sichuan, 637000, China

³ School of Basic Medical Sciences and Forensic Medicine, North Sichuan Medical College, Fujiang Road 234, Nanchong City, Sichuan, 637000, China

⁴ Department of Stomatology, North Sichuan Medical College, Fujiang Road 234, Nanchong City, Sichuan, 637000, China

⁵ Department of Cardiovascular disease, School of Clinical Medicine, Affiliated Hospital of North Sichuan Medical College, Maoyuan Road 1, Nanchong City, Sichuan, 637000, China.

§ These authors contribute equally

* Corresponding Author(s): Haiying Wang, hywang@nsmc.edu.cn; Jiang Zhu, zhujiang@nsmc.edu.cn

Table of Contents

1. **Figure S1.** Photograph of aqueous solutions of MnL, TiL_3Mn_3 and FeL_3Mn_3 (pH = 7.4).
2. **Figure S2.** Photograph of FeL_3Mn_3 at pH = 7.4 and 9.0 (in Tris buffer, 0.1 M)
3. **Figure S3.** The stability of FeL_3Mn_3 in the presence of 10 % FBS (at 37 °C) and the PBS solution (pH = 7.4, 10 mM) of FeL_3Mn_3 was employed as the negative control.
4. Photothermal conversion efficiency measurement of FeL_3Mn_3 .
5. **Figure S4.** $^1\text{O}_2$ quantum yield measurement of FeL_3Mn_3 .
6. **Figure S5.** Hyperthermia heating curves of BxPC-3 cells media with FeL_3Mn_3 at various concentrations (0, 0.125, 0.25, 0.5 mM) under 808 nm laser (2 W cm^{-2}) irradiation for 6 min.
7. **Figure S6.** The change of absorption spectra of DPBF (20 μM) mixed with FeL_3Mn_3 (120 μM) over time without (a) / with (b) ascorbate sodium (1.0 mM) under 808 nm laser irradiation (2.0 W cm^{-2})

1. Photograph of aqueous solutions of three chelates.

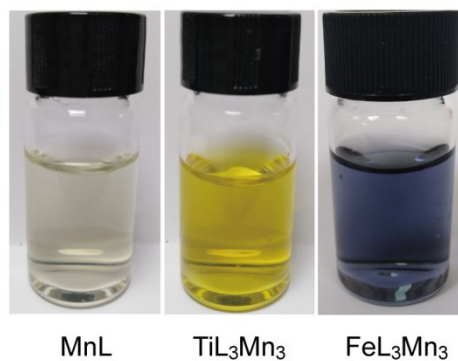


Figure S1 Photograph of aqueous solutions of MnL, TiL_3Mn_3 and FeL_3Mn_3 (pH = 7.4).

2. Photograph of FeL_3Mn_3 at different pH condition.



Figure S2 Photograph of FeL_3Mn_3 at pH = 7.4 and 9.0 (in Tris buffer, 0.1 M).

3. Stability of FeL₃Mn₃ in different mediums

4. Photothermal conversion efficiency measurement of FeL₃Mn₃.

To calculate the photothermal conversion efficiency (η) of FeL₃Mn₃, the FeL₃Mn₃ solution (0.25 mM, 0.3 ml, in HEPES buffer, pH = 7.4, 0.1 M) was irradiated by 808 nm laser (2.0 W cm⁻²) for 10 min, and then the laser was shut off. The solution was naturally cooled to room temperature. The η was calculated according to a previously described method:

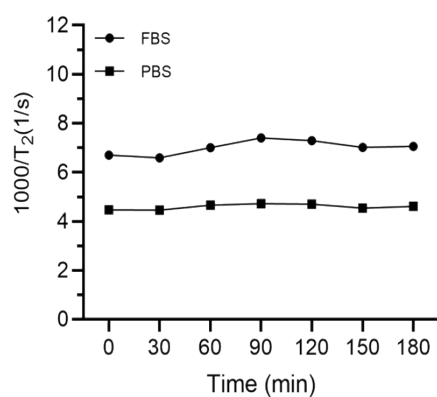


Figure S3 The stability of FeL₃Mn₃ (0.2 mM) in the presence of 10 % FBS (at 37 °C) and the PBS solution (pH = 7.4, 10 mM) of FeL₃Mn₃ was employed as the negative control.

$$\eta = \frac{hs(T_{Max} - T_{Surr}) - Q_{Dis}}{I(1 - 10^{-A808})} \quad (A1)$$

$$hs = \frac{mC}{\tau_s} \quad (A2)$$

$$t = -\tau_s \ln(\theta) \quad (A3)$$

$$\theta = \frac{T - T_{Surr}}{T_{Max} - T_{Surr}} \quad (A4)$$

h represents the heat transfer coefficient,

s represents the surface area of the container,

h_s can be determined from the equation (A2),

T_{Max} represents the maximum steady state temperature,

T_{Surr} represents the ambient room temperature,

Q_{Dis} represents heat dissipated from the laser mediated by the solvent and container,

I represent the laser power and A is the absorbance at 808 nm.

m represents the mass of the solution (g) containing the photoactive material,

C approximate to the specific heat capacity of water,

τ_s represents the associated time constant, which can be determined from the equation (A3),

t represents the time required to cool to room temperature,

θ represents the driving force temperature, which be calculated from the equation (A4),

T represents instantaneous temperature during cooling.

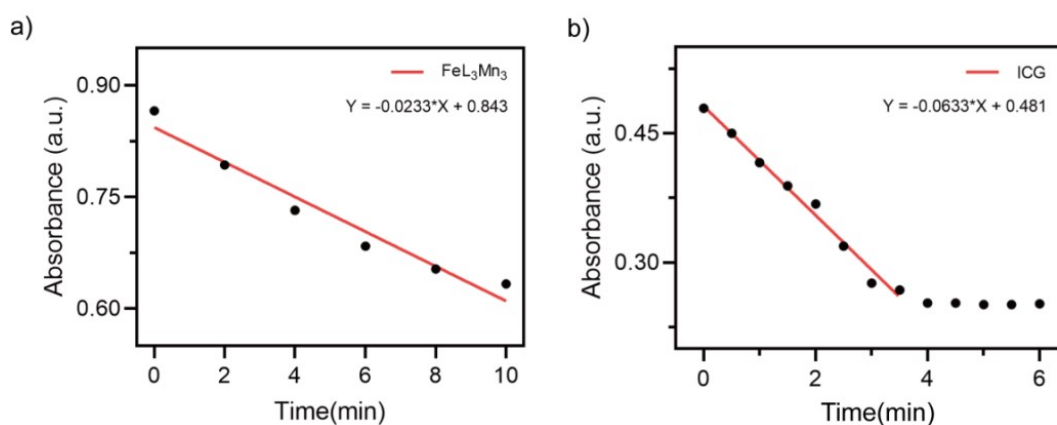


Figure S4 $^1\text{O}_2$ quantum yield measurement of FeL₃Mn₃. a) Decrease in absorbance intensity of DPBF recorded at 410 nm in the presence of FeL₃Mn₃ as a function of irradiation time. b) Decrease in absorbance intensity of DPBF recorded at 410 nm in the presence of indocyanine green (ICG) as a function of irradiation time.

5. $^1\text{O}_2$ quantum yield measurement of FeL₃Mn₃.

When indocyanine green was selected as the reference compound ($\Phi_{\Delta\text{ICG}} = 0.14$ in water), the

$^1\text{O}_2$ yield of FeL₃Mn₃ was calculated by the following equation: $\Phi_{\Delta\text{S}} = \Phi_{\Delta\text{ICG}} \cdot (k_{\text{S}} \cdot F_{\text{ICG}}) / (k_{\text{ICG}} \cdot F_{\text{S}})$,

where superscript S and ICG represent the FeL₃Mn₃ and ICG respectively. k is the DPBF photobleaching rates (410nm). F is the absorption correction factor, which can be calculated

from $F = 1 - 10^{-\text{OD}}$ (OD is the absorbance of samples at 808 nm).

6. Photothermal effect of FeL_3Mn_3 on BxPC-3 cells.

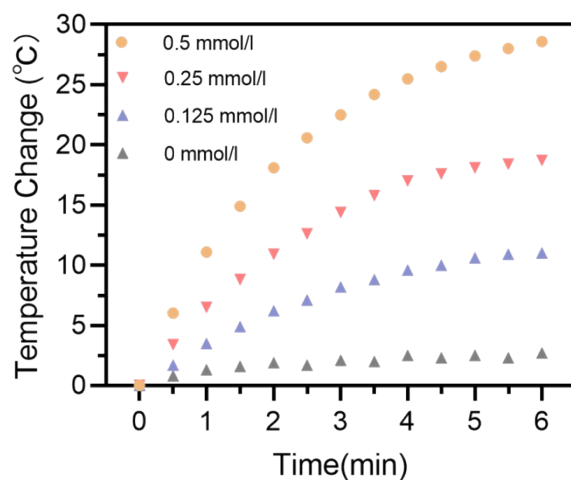


Figure S5 Hyperthermia heating curves of BxPC-3 cells media with FeL_3Mn_3 at various concentrations (0, 0.125, 0.25, 0.5 mM) under 808 nm laser (2 W cm^{-2}) irradiation for 6 min.

7. Shielding of the photodynamic effect of FeL_3Mn_3 .

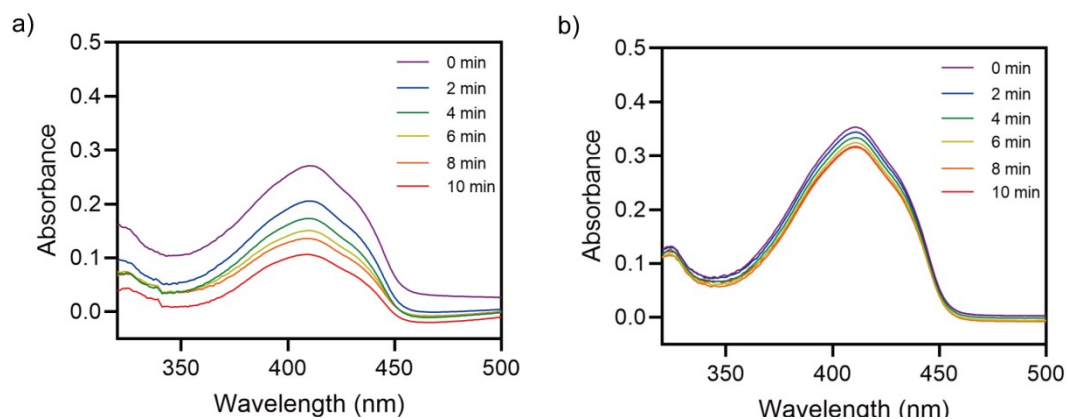


Figure S6 The change of absorption spectra of DPBF ($20 \mu\text{M}$) mixed with FeL_3Mn_3 ($120 \mu\text{M}$) over time without (a) / with (b) ascorbate sodium (1.0 mM) under 808 nm laser irradiation (2.0 W cm^{-2})